Protein Engineering, Design & Selection vol. 23 no. 10 pp. 769–780, 2010
Published online August 9, 2010 doi:10.1093/protein/gzq051

A chemically modified α-amylase with a molten-globule state has entropically driven enhanced thermal stability†

Khawar Sohail Siddiqui[1,6], Anne Poljak[2,3], Davide De Francisci[1], Gea Guerriero[1,5], Oliver Pilak[1], Dominic Burg[1], Mark J.Raftery[2], Don M.Parkin[4], Jill Trewhella[4] and Ricardo Cavicchioli[1]

[1]School of Biotechnology and Biomolecular Sciences, [2]Bioanalytical Mass Spectrometry Facility, [3]School of Medical Sciences, University of New South Wales, Sydney, NSW 2052, Australia, [4]School of Molecular Biosciences, University of Sydney, Sydney, NSW 2006, Australia and [5]Present address: Department of Glycoscience, KTH, Royal Institute of Technology Alba Nova University Centre, SE-106 91 Stockholm, Sweden

[6]To whom correspondence should be addressed. E-mail: k.siddiqui@unsw.edu.au

Received April 12, 2010; revised June 29, 2010; accepted July 15, 2010

Edited by Pang-Chui Shaw

The thermostability properties of TAA were investigated by chemically modifying carboxyl groups on the surface of the enzyme with AMEs. The TAA_{MOD} exhibited a 200% improvement in starch-hydrolyzing productivity at 60°C. By studying the kinetic, thermodynamic and biophysical properties, we found that TAA_{MOD} had formed a thermostable, MG state, in which the unfolding of the tertiary structure preceded that of the secondary structure by at least 20°C. The X-ray crystal structure of TAA_{MOD} revealed no new permanent interactions (electrostatic or other) resulting from the modification. By deriving thermodynamic activation parameters of TAA_{MOD}, we rationalised that thermostabilisation have been caused by a decrease in the entropy of the transition state, rather than being enthalpically driven. Far-UV CD shows that the origin of decreased entropy may have arisen from a higher helical content of TAA_{MOD}. This study provides new insight into the intriguing properties of an MG state resulting from the chemical modification of TAA.

Keywords: activation thermodynamics/calorimetry/entropy/enzyme kinetics/protein X-ray crystallographic structure

Introduction

As a general principle, enzymes from thermophilic organisms tend to be thermostable, whereas those from psychrophiles tend to be thermolabile. There also tends to be a trade-off between enzyme activity and stability (Siddiqui and Cavicchioli, 2006). When compared at the same temperature, enzymes from thermophiles typically exhibit higher thermostability but lower activity than those from psychrophiles.

The types of structural features that can affect the thermostability/thermolability of proteins are well-documented. For example, high thermostability is associated with large numbers of electrostatic interactions, short and rigid surface loops, a large number and tight metal-binding sites, high packing density and core hydrophobicity, higher secondary structure and a reduced conformational or solvation entropy of the unfolded state (Petsko, 2001; Vieille and Zeikus, 2001; Eijsink *et al*., 2004; Siddiqui and Cavicchioli, 2006; Daniel *et al*., 2008). Despite this general knowledge, it remains a difficult task to predict from a protein sequence (i.e. in the absence of empirical testing) which structural features play the most critical roles in promoting thermostability. As a consequence, it is a challenge to adopt a rational approach (e.g. peptide synthesis, site-directed mutagenesis) to enzyme engineering for optimising the thermal properties of an enzyme, and methods that broadly screen for improvements (e.g. directed evolution or chemical modification) tend to be more fruitful.

Using directed evolution and chemical modification, the specific activity and thermostability of a lipase were both increased, illustrating that the trade-off between activity and stability can, in some circumstances, be overcome (Zhang *et al*., 2003; Siddiqui and Cavicchioli, 2005). Novel mechanistic understanding about temperature-dependent activity has also been obtained for a protease, using chemical modification and a range of kinetic and biophysical analyses (Siddiqui *et al*., 2009). In this case, low temperature activity of the protease was increased by reducing uncompetitive substrate inhibition. These examples illustrate the scope that is available for continuing to uncover fundamental properties of enzyme thermostability/activity, as well as the biotechnological advances that can be achieved using this knowledge.

One aspect of protein stability that has received little attention as a mechanism for affecting or manipulating thermostability relates to intermediate and unfolded states of proteins (Matsumura *et al*., 1989; Shortle, 1996). Proteins can adopt a continuum of interconvertible states ranging from ordered (folded state) to intermediate (MG) to unfolded (or random-coil; Uversky, 2002). An MG is an intermediate state that has a substantial secondary structure but reduced tertiary structure, lacks rigid side-chain packing and has a high degree of solvent accessibility of hydrophobic residues (Ptitsyn, 1995; Wang *et al*., 1998; Koshiba *et al*., 2000; Cox *et al*., 2003; Mizuguchi *et al*., 2005). The MG state can be induced by the extremes of pH or salt concentrations, the presence of denaturing agents, elevated temperature or chemical modification (Dolginova *et al*., 1992). The molecular dimensions of MG states and the forces that stabilise them are not well understood. Studies examining MGs have mainly been performed with relatively small proteins, including α-lactalbumin, cytochrome *c*, apomyoglobin and lysozyme (Ptitsyn, 1996; Mizuguchi *et al*., 2005), with very few studies examining large multidomain proteins.

†The structure factors and atomic coordinates of modified Taka-amylase have been deposited in the PDB under accession code 3KWX.

Recently, a low-pH-induced MG state was described for α-amylases from mesophilic and thermophilic species of *Bacillus* (Shokri *et al*., 2006). TAA (1,4-α-D-glucan glucanohydrolase, EC 3.2.1.1) from the fungus *Aspergillus oryzae* (TAA) is a model α-amylase that is structurally and biophysically well characterised (Brzozowski and Davies, 1997) and is used commercially for a range of industrial applications (Mitidieri *et al*., 2006). TAA has a $(\alpha/\beta)_8$ TIM barrel architecture and is a multidomain monomeric protein (Janecek and Baláz, 1992), which unfolds irreversibly at moderate (50–55°C) temperatures (Eijsink *et al*., 2004).

For industrial applications of α-amylases, useful reaction conditions include pH 4.5–5.0, no added Ca^{+2} and high temperatures (Richardson *et al*., 2002). The optimal conditions for TAA are pH 5 and no Ca^{+2} (Chang *et al*., 1995). However, TAA lacks thermostability. In this study, we explored the thermostability properties of TAA by performing chemical modification with AME to modify carboxyl groups on the surface of the enzyme (Scheme 1). Arginine residues tend to be favoured over lysine residues in proteins from thermophilic organisms and are thought to enhance stability through the ability of the guanidinium side chain to form multiple electrostatic interactions, including salt bridges, hydrogen bonds (Mrabet *et al*., 1992; Siddiqui and Cavicchioli, 2005; Siddiqui *et al*., 2006) and Arg–pi interactions (Gallivan and Dougherty, 1999). Arginine residues have also been linked to the ability to facilitate the formation of an MG state (Xie *et al*., 2004). By studying the kinetic, thermodynamic and biophysical properties of the AME-TAA_{MOD}, we found that it was capable of forming a thermostable MG state. This increased thermostability was directly related to an enhanced productivity of the TAA_{MOD}.

Materials and methods

Protein estimation

Total protein was estimated using a NanoDrop ND-1000 Spectrophotometer and the conversion, A_{280} 1.9 = 1 mg ml^{-1}. The extinction coefficient was determined by computing Taka-amylase protein sequence using the ProtParam tool (www.expasy.org/tools/protparam.html).

Chemical modification

The carboxyl groups of TAA (Megazyme International, Ireland) were activated by EDC hydrochloride in the presence of a nucleophile, AME 2HCl (Siddiqui *et al*., 1993; Walker, 2002; Cavicchioli *et al*., 2006). A nucleophile solution, containing K_2HPO_4/KH_2PO_4 (0.04 M, pH 5.4), AME 2HCl (1 M), NaCl (0.01 M) and maltose (0.05 M), was prepared and pH readjusted to 5.22 with 10 M NaOH. TAA (40 mg) in 10 mM aqueous NaCl solution was added to the nucleophile solution and the volume adjusted to 80 ml with water. EDC (50 mM) was added to initiate the reaction and after 30 min, sodium acetate/acetic acid (0.05 M, pH 7) was added to quench the reaction. TAA_{MOD} and TAA_{UM} were dialysed against 0.01 M Tris–HCl, 0.05 M $CaCl_2$ (pH 7.5), concentrated to ~10 mg ml^{-1} using Millipore Filtration Units (cut-off, 5 kDa), frozen in liquid N_2 and stored at −80°C. For all experiments except X-ray crystallography, both samples were dialysed against sodium acetate buffer (50 mM, pH 5) to produce Ca^{+2}-depleted amylases (Fukada *et al*., 1987; Duy and Fitter, 2005).

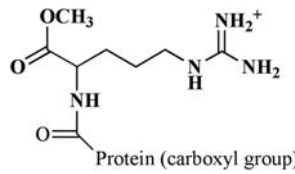

Scheme 1. Chemical modification of carboxyl group of protein with AME.

Ion-exchange chromatography

TAA_{UM} and TAA_{MOD} were characterised using anion-exchange (Resource-15Q) and cation-exchange (Resource-15S) chromatography columns (10 × 100 mm) fitted to an AKTA Basic Liquid Chromatography System (GE Healthcare, Australia). The system was controlled by Unicorn Software and both columns were equilibrated in buffer A (0.02 M MES, pH 6.5) at a flow rate of 4 ml min^{-1} using a 0.5 ml sample loop. Equal amounts (0.8 mg) of both proteins were loaded onto each column using 500 and 100 μl loops for TAA_{UM} and TAA_{MOD}, respectively. Proteins were eluted using a gradient (buffer A containing 1 M NaCl) from 0 to 1 M NaCl in 25 min.

Non-denaturing PAGE

Both proteins (5 μg) were subjected to 7.5% non-denaturing PAGE employing 20 mM CAPS/NH_4OH, pH 10.6, buffer in the resolving gel, tank buffer and sample buffer and without a stacking gel.

Mass spectrometry

The masses of intact (TAA_{UM} and TAA_{MOD}) amylases were determined by MALDI-TOF-MS, as were the peptide mass fingerprints, generated by tryptic, endoaspN, endolysC and argC cleavage (Stanley and Poljak, 2003; Siddiqui *et al*., 2004; Siddiqui *et al*., 2006; for details, see Supplementary data). Amylases were desalted using C4 ziptips and eluted directly onto a stainless steel target, using solvent (80% CH_3CN, 0.1% TFA) containing caffeic acid matrix (10 mg/ml). A Voyager DE STR mass spectrometer (Applied Biosystems, Framingham, MA, USA) was used for MALDI-TOF analyses. Data acquisition was performed in the positive ion mode and the instrument calibrated immediately prior to each analysis. For the analysis of intact control and TAA_{MOD}, calmix 3 was used with caffeic acid matrix and the average masses of the singly protonated molecular ions of bovine insulin ($[M + H]^+ = 5734.59$), *Escherichia coli* thioredoxin ($[M + H]^+ = 11\,674.48$) and equine apomyoglobin ($[M + H]^+ = 16\,952.56$) were used to calibrate the mass axis. Linear delayed extraction mode was used, acquiring 100 averaged spectra for each analysis. Spectra of intact amylases were processed by baseline correction, noise removal (2 SD) and Gaussian smoothing (SM165) using the Voyager Data Explorer Software.

Circular dichroism

Far-UV spectra in the range 190–260 nm (20°C) and thermal unfolding curves at 222 nm (0.05 M sodium acetate, pH 5) were recorded using TAA_{UM} and TAA_{MOD} (Fitter, 2005). Temperature-induced unfolding of secondary structure was monitored using a JASCO J-810CD Spectropolarimeter under constant nitrogen flow, connected to a Peltier temperature controller. The temperature was varied from 30°C to 100°C at a

rate of 15°C or 60°C h^{-1}. Spectra were recorded using a 0.1 cm path length and protein concentrations of 3.8 and 3.6 μM for TAA_{UM} and TAA_{MOD}, respectively. Spectra were corrected for the buffer signal. To determine T_m, the fraction unfolded was plotted versus temperature (Cavicchioli *et al*., 2006).

Differential scanning calorimetry

Both proteins were dialysed against sodium acetate buffer (50 mM, pH 5) using dialysis tubing (12 kDa cut-off). Thermograms of the dialysed (1 mg ml^{-1}) samples (TAA_{UM}, 19 μM; TAA_{MOD}, 18 μM) were recorded using a Microcal VP-DSC with a cell volume of 0.5072 ml and 2 atm pressure. Prior to scanning, all solutions were degassed by stirring under vacuum for 15 min. Scans were performed by increasing the temperature from 10°C to 120°C at 60°C h^{-1}. Thermograms were analysed using Origin Software. The apparent T_m was determined as the temperature corresponding to maximum C_p, and the rate constant for unfolding (k_{unfol}) was calculated:

$$k_{unfol} = \frac{vC_p}{Q - Q_T} \quad (1)$$

where v is the scan rate (1°C min^{-1}), C_p the excess heat capacity at a given temperature T, Q the total heat of the process and Q_T the heat evolved at a given temperature (Sanchez-Ruiz *et al*., 1988; D'Amico *et al*., 2003; Cavicchioli *et al*., 2006):

$$\text{Half-life of unfolding}(t_{1/2\text{-unfol}}) = \ln 2/k_{unfol} \quad (2)$$

Activation thermodynamics for kinetic stability

The thermodynamic activation parameters for the kinetic stability of TAA_{UM} and TAA_{MOD} were determined (Segal, 1993; Oliveberg *et al*., 1995; Siddiqui *et al*., 2002; D'Amico *et al*., 2003), using

$$\Delta G^{\ddagger}(\text{free energy of activation}) = -\text{RT}\ln\left(\frac{k_{unfol} \times h}{k_B \times T}\right) \quad (3)$$

where R is the universal gas constant (8.314 J K^{-1} mol^{-1}), T the absolute temperature, k_{unfol} the first-order rate constant of unfolding determined by DSC, h the Planck constant (6.63×10^{-34} J s) and k_B the Boltzman constant (1.38×10^{-23} J K^{-1})

$$\Delta H^{\ddagger}(\text{enthalpy of activation}) = E_a - \text{RT} \quad (4)$$

where E_a is the activation energy determined from the slope of an Arrhenius plot by plotting ln k_{unfol} versus $1/T$ (Siddiqui *et al*., 2002)

$$\Delta S^{\ddagger}(\text{entropy of activation}) = \frac{\Delta H^{\ddagger} - \Delta G^{\ddagger}}{T} \quad (5)$$

Irreversible thermal inactivation

Appropriately diluted TAA_{UM} and TAA_{MOD} were incubated in sodium acetate/acetic acid buffer (0.05 M, pH 5) at various temperatures. Aliquots were withdrawn at time intervals, cooled on ice and residual enzyme activity determined (see the 'Enzyme assays' section below). The data were fitted to the first-order plots and half-lives of thermal inactivation ($t_{1/2\text{-inact}}$) were determined using Equation (2) (Chang *et al*., 1995; Siddiqui *et al*., 2004).

ANS-fluorescence melting curves

All fluorescence studies were carried out using a Perkin–Elmer LS 50B fluorescence Spectrofluorimeter fitted with a Perkin–Elmer peltier temperature controller. Sodium acetate buffer (2 ml; 0.05 M, pH 5) containing 45 μg ml^{-1} (0.86 μM) and 41 μg ml^{-1} (0.75 μM) of TAA_{UM} and TAA_{MOD}, respectively, was equilibrated at 20°C. ANS (5 μl; 10 mM) in methanol was added to the protein solution with constant magnetic stirring. The protein was excited at 380 nm, and the emission spectra were acquired from 460 to 560 nm using excitation and emission slit widths of 5 nm at a scan rate of 100 nm min^{-1}. Spectra were acquired at temperatures up to 70°C. The reference spectrum (buffer plus ANS) at each temperature was subtracted from the respective protein spectrum. The intensity corresponding to 480 nm was plotted against temperature for both TAA_{UM} and TAA_{MOD} (Cox *et al*., 2003).

Urea fluorescence unfolding curves

Unmodified (0.21 μM) and modified (0.20 μM) proteins were excited at 295 nm and emission spectra acquired from 310 to 380 nm at a scan rate of 100 nm min^{-1}. The experiment was carried out in sodium acetate buffer (0.05 M, pH 5) with urea added in 0.5 M increments across the 0–9.5 M concentration range. Urea unfolding curves of TAA_{UM} and TAA_{MOD} were generated at 40°C by plotting fraction unfolded (using emission intensity at 330 nm) versus urea concentration (Wang *et al*., 1998; Cavicchioli *et al*., 2006).

Dynamic fluorescence quenching

TAA_{UM} and TAA_{MOD} were excited at 280 nm and the fluorescence intensities of Trp/Tyr residues emitted at 350 nm were recorded in the presence of increasing amounts of a small quencher molecule (acrylamide) at 10°C, 35°C, 40°C and 45°C (Fitter, 2005; Cavicchioli *et al*., 2006; Siddiqui and Cavicchioli, 2006; Siddiqui *et al*., 2009). The slopes corresponding to the Stern–Volmer constants were determined using Microcal Origin 5.0.

Enzyme assays

Amylase activity was determined by measuring reducing sugars released from starch (Chang *et al*., 1995). Appropriate amounts of amylase solution (20–100 μl) were added to 1 ml of 2% (w/v) potato starch solution in sodium acetate/acetic acid buffer (0.05 M, pH 5) at 45°C. After 10 min, the reaction was terminated by adding 1 ml of dinitrosalicylic acid reagent, the mixture was boiled for 5 min, cooled, centrifuged at 21 000*g* for 12 min, and A_{540} was measured against the reagent blank. The A_{540} units were converted to units per milligram protein using a maltose standard curve. To generate productivity curves of TAA_{UM} and TAA_{MOD}, the hydrolysis of starch was determined at 60°C. Substrate solution (potato starch, 17 ml, 6% w/v in 0.05 M sodium acetate/acetic acid, pH 5) was aliquoted in 50 ml centrifuge tubes and incubated at 60°C. The hydrolysis reaction was initiated by the addition of 5.5 μg of enzyme. To determine non-enzymatic hydrolysis, buffer was added to the substrate

solution and incubated at the same temperature (reagent blank). After appropriate time intervals, 0.5 ml aliquots were withdrawn in triplicate and assayed.

Kinetic parameters for starch hydrolysis

Michaelis–Menten kinetic parameters (k_{cat} and K_m) of TAA_{UM} and TAA_{MOD} were determined. The enzyme was incubated in sodium acetate buffer (0.05 M, pH 5) containing different amounts of starch (0.01–0.1% w/v) at 40°C and assayed for 15 min (Chang *et al*., 1995). The data were fitted directly to the Michaelis–Menten plots using the Enzyme Kinetics Module 1.1 linked to Sigma Plot 8.02.

Effect of temperature on the hydrolysis of starch

TAA_{UM} and TAA_{MOD} were incubated in sodium acetate/acetic acid buffer (0.05 M, pH 5) containing 2% (w/v) starch and assayed for 10 min at various temperatures to determine activation energies (E_a). The data were plotted, analysed and thermodynamic activation parameters, $\Delta G^{\ddagger}$, $\Delta H^{\ddagger}$ and $\Delta S^{\ddagger}$ determined using Equations (3) and (4) (by substituting k_{cat} in lieu of k_{unfol}) and Equation (5), respectively (Siddiqui *et al*., 2002). Optimum temperature (T_{opt}) was determined as the temperature corresponding to the maximal activity.

Small-angle X-ray scattering

TAA_{UM} and TAA_{MOD} (12.5 mg ml^{-1}) were mixed with a solution of 10 M urea to give a final protein concentration of 5 mg ml^{-1} (TAA_{UM}, 95 μM; TAA_{MOD}, 90 μM) in sodium acetate/acetic acid buffer (0.05 M, pH 5) and final urea concentrations of 0, 3 and 6 M. Thirty microlitre samples were used for each analysis. SAXS data were acquired using an Anton Paar SAXSess instrument with data reduction and analysis protocols as described previously (Jeffries *et al*., 2008). A CCD detector was used and the sample temperature control set to maintain the sample at 25°C. Predicted structural parameters based on crystal structure coordinates of the TAA_{UM} (PDB: 7TAA) were evaluated using CRYSOL (Svergun *et al*., 1995). $P(r)$ functions were calculated using the indirect Fourier transformation methods encoded in GNOM (Svergun, 1992) and GIFT (Fritz *et al*., 2000). Four sequential 15 min data acquisitions were conducted on each sample to accumulate sufficient statistics and to enable the evaluation of sample stability during the experiments. Aggregation was observed in the modified protein samples (TAA_{MOD}) after the first 15 min acquisition; subsequent data analysis for this sample did not include the data from later acquisitions.

Although additional measurements were made with different concentrations of urea (0 and 3 M for TAA_{MOD}, and 3 and 6 M urea for TAA_{UM}) and at 40°C, these other conditions all gave rise to aggregation that precluded structural analysis. In the case of samples analysed here, $I(0)$ analysis demonstrated that the TAA_{MOD} samples in 6 M urea had no aggregation.

X-ray diffraction analysis

TAA_{MOD} (10 mg ml^{-1} in 10 mM Tris, pH 7.5, containing 5 mM $CaCl_2$) was crystallised at 20°C by vapour diffusion against a solution of 20% polyethylene glycol 4000, 0.4 M ammonium sulphate and 0.1 M MES, pH 7.2. Single crystals with a regular morphology (150 × 150 × 300 μm) grew after 2 weeks. Crystals were transferred into a cryoprotectant consisting of the crystallisation solution plus 7–12% glycerol. Diffraction data were collected at 100 K on beam line 23-ID-D at the Advanced Photon Source, Argonne National Laboratory using a MarMosaic 300 CCD detector with a wavelength of 0.98 Å. Data were reduced and scaled using the CCP4 suite of programs (Collaborative Computational Project, 1994). The structure was solved by molecular replacement using the software Phaser (McCoy *et al*., 2007) with the coordinates of the wild-type enzyme (PDB: 2GVY; Vujicic-Zagar and Dijkstra, 2006) as a search model. Model rebuilding was carried out using COOT (Emsley and Cowtan, 2004) and the structure was refined using the program PHENIX (Adams *et al*., 2002). Only protein atoms (Ala1 to Ser476), one bound calcium ion and a single *N*-acetyl-D-glucosamine modification of Asn197 and 261 ordered water molecules were included in the refinement (final R-factor of 0.176 with an R-free of 0.211). Data reduction and refinement statistics are given in Supplementary Table SI. Sites of chemical modification were determined by visual inspection of difference electron density maps. Chemical modifications were not sufficiently ordered or populated to warrant inclusion in the atomic model. The atomic coordinates were deposited in PDB (accession code 3KWX).

Results

Chemical modification of TAA

The largest overt effect of the AME modification is a change in charge caused by the conversion of negatively charged carboxyl groups to positively charged AME groups (Scheme 1). Ion-exchange chromatography (pH 6.5) demonstrated the binding of TAA_{UM} (Fig. 1A, high intensity, sharp peak) to anion-exchange resin and TAA_{MOD} (Fig. 1A, low intensity, broad peak) to cation-exchange resin; i.e. TAA_{MOD} acquired a higher pI than TAA_{UM}. Similarly, the non-denaturing gel (Fig. 1A, inset) also showed that TAA_{MOD} (right lane) has a higher pI than TAA_{UM} (left lane).

The broadness of the protein peak in the chromatogram (Fig. 1A) and the streaky protein band in the non-denaturing gel (Fig. 1A, inset, right lane) are both indicative of charge heterogeneity in the modified enzyme. As revealed by MALDI-TOF-MS of the intact protein (Fig. 1B) and SDS–PAGE (Fig. 1B, inset), the linking of AME moieties to the carboxyl groups of TAA also generated a small increase in the molecular weight of TAA_{MOD}, with an average mass shift of 2096 Da.

TAA contains 54 carboxyl groups (C-terminus plus 41 Asp and 12 Glu) that can potentially link to AME (mass shift, 170.12 Da). Spontaneous hydrolysis of the AME ester group can also lead to the formation of arginine (mass shift, 156.10 Da). A total mass increase of ~2096 Da was observed for TAA_{MOD} (Fig. 1B), indicative of an average extent of modification of 12–13 carboxyl groups. Chemically modified sites identified by MALDI-TOF-MS and LC-MS/MS are presented in Supplementary Table SII.

Modification improves protein stability

Irreversible thermal inactivation and thermal denaturation were interpreted according to the general model of Lumry

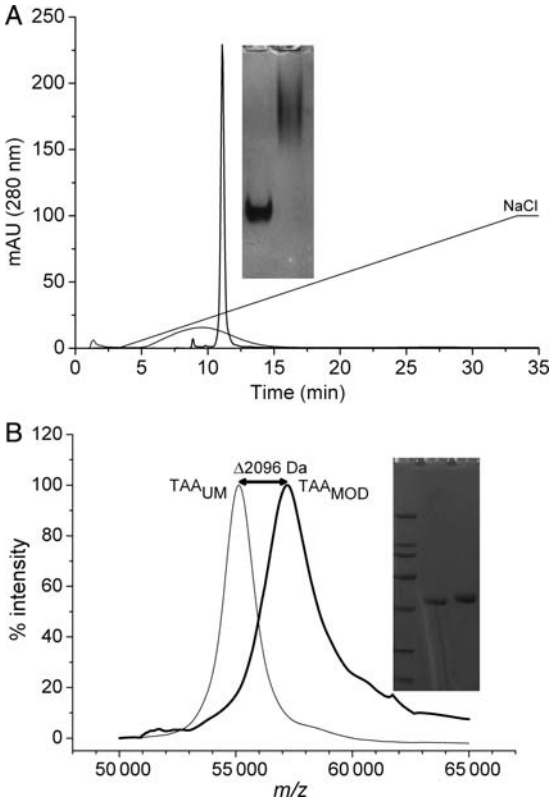

Fig. 1. Analysis of charge and size characteristics of TAA_{UM} and TAA_{MOD}. (**A**) Anion-exchange chromatography of TAA_{UM} at pH 6.5 (intense and sharp peak) and cation-exchange chromatography of TAA_{MOD} at pH 6.5 (small and broad peak). Inset, non-denaturing PAGE of TAA_{UM} (left) and TAA_{MOD} (right). (B) MALDI-TOF-MS used for examining the extent of modification of undigested TAA_{UM} and TAA_{MOD}. Inset, SDS–PAGE of TAA_{UM} (middle) and TAA_{MOD} (right) using 4–20% gradient gel. Molecular weights of marker proteins (left) are from top to bottom, 200, 116, 97, 66, 45, 31 and 21 kDa.

and Eyring applied on α-amylases as follows (Violet and Meunier, 1989; Fitter, 2005):

$$N \underset{k_{-1}}{\overset{k_1}{\leftrightarrow}} U \xrightarrow{k_2} D \qquad (6)$$

where N is the native enzyme, U the reversibly unfolded state, D the irreversibly denatured final state and k_1 and k_2 the rate constants. Thermal stability strongly depends on the magnitude and relation of the different rate constants (Sanchez-Ruiz *et al*., 1988; Fitter, 2005). Initially, activity is reversibly lost due to the disruption of the non-covalent interactions (N ↔ U). Enzyme activity is completely recovered when the enzyme is cooled down. Prolonged heating at high temperatures then leads to an irreversibly inactivated and aggregated enzyme (D).

The half-life of inactivation ($t_{1/2\text{-inact}}$) and half-life of unfolding ($t_{1/2\text{-unfol}}$) were determined (Table I). At a temperature approximating T_{opt} (50°C), TAA_{MOD} had a 28-fold higher $t_{1/2\text{-inact}}$ compared with TAA_{UM}. The values for $t_{1/2\text{-inact}}$ of TAA_{UM} for the temperatures tested between 50°C and 60°C (Supplementary Fig. S1) were similar to the values for $t_{1/2\text{-unfol}}$ (Table I), and the published value for TAA_{UM} at 50°C (Chang *et al*., 1995). In contrast, although the $t_{1/2\text{-unfol}}$ values for TAA_{MOD} were higher than TAA_{UM}, the $\Delta t_{1/2}$ at 50°C was only ~2-fold (i.e. compared with 28-fold for $\Delta t_{1/2\text{-inact}}$).

Table I. Irreversible thermal inactivation and unfolding of TAA_{UM} and TAA_{MOD}

Temperature (°C)	Inactivation[a] ($t_{1/2\text{-inact}}$, min)		Unfolding[b] ($t_{1/2\text{-unfol}}$, min)	
	TAA_{UM}	TAA_{MOD}	TAA_{UM}	TAA_{MOD}
50	12 ± 1 (27)	340 ± 84	10	22
53	6 ± 0.5	140 ± 23	6	17
55	4 ± 0.30	30 ± 30	4	14
60	1 ± 0.30	6 ± 0.35	—	8

[a]Inactivation parameters determined using starch hydrolyzing assay (Supplementary Figure S1). The value in parenthesis was taken from Chang *et al*. (1995). [b]Unfolding of tertiary structure using DSC.

Interestingly, the $t_{1/2\text{-unfol}}$ of TAA_{MOD} is significantly less than the $t_{1/2\text{-inact}}$ at temperatures of 50°C, 53°C and 55°C (Table I). During unfolding of TAA_{MOD} as measured by DSC, $k_2 >> k_{-1}$ so that at any moment most of the U molecules will be denatured to D instead of refolding to the native state (N) and thus denaturation may be considered a two-state irreversible process (Sanchez-Ruiz *et al*., 1988)

$$N \xrightarrow{k_2} D \qquad (7)$$

Conversely, within the context of thermal inactivation, these results can be understood if we assume that $k_2 << k_{-1}$ so that the majority of partially unfolded TAA_{MOD} are refolded to N state upon cooling and regain activity (Violet and Meunier, 1989). The irreversible step may nonetheless be faster at higher temperatures such that the $t_{1/2\text{-inact}}/t_{1/2\text{-unfol}}$ ratio of TAA_{MOD} decreases with increase in temperature (15, 8 and 2 at 50°C, 53°C and 55°C, respectively), becoming equal at 60°C.

The fluorescence spectra of TAA_{UM} and TAA_{MOD} were determined in the presence of a range of urea concentrations at 40°C (Supplementary Fig. S2), and $[urea]_{1/2}$ (urea concentration at which 50% of native structure is lost) calculated from the decrease in fluorescence emission intensity at 330 nm (Fig. 2A, Table II). TAA_{MOD} showed greater resistance to urea unfolding compared with TAA_{UM} ($\Delta[urea]_{1/2}$, 1.3 M).

Dynamic fluorescence quenching of Tyr/Trp residues by acrylamide was used to assess the flexibility and the integrity of TAA_{UM} and TAA_{MOD}. Low temperature (10°C) was used to minimize protein unfolding and maximize the capacity to probe the inherent flexibility of the protein. Higher temperatures (35–45°C) were used to assess overall structural integrity. At 10°C, the Stern–Volmer quenching constants (K_{SV}: $16 \pm 0.3\ M^{-1}$) calculated from the Stern–Volmer plots (Fig. 2B) for TAA_{MOD} and TAA_{UM} were similar, indicating that acrylamide penetration to the interior of the protein was equivalent in both proteins. At acrylamide concentrations >0.05 M as the temperature was increased from 35°C to 45°C, the slopes of the curves for TAA_{UM} progressively increased compared with TAA_{MOD}. The upward curvature of the Stern–Volmer plots at higher acrylamide concentrations is indicative of Trp residue exposure and complete quenching during unfolding (Fitter and Haber-Pohlmeier, 2004).

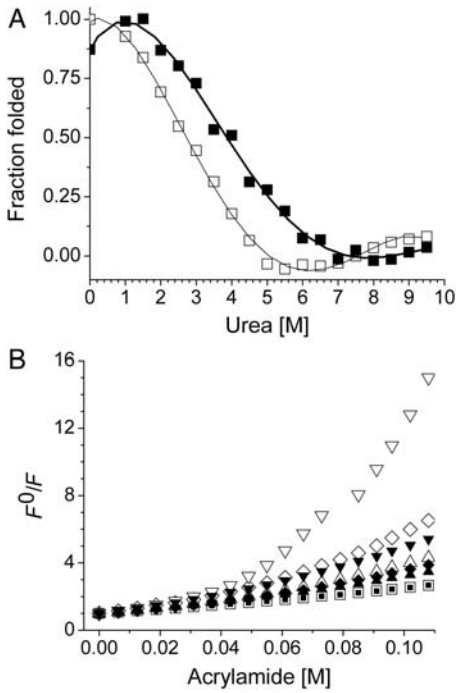

Fig. 2. Stability and flexibility of TAA_{UM} and TAA_{MOD}. Open symbols or thin line, TAA_{UM}; closed symbols or thick line, TAA_{MOD}. (**A**) Urea unfolding curves using intrinsic fluorescence to assess tertiary structure stability; (**B**) Dynamic fluorescence quenching using acrylamide at 10°C (squares), 35°C (triangles), 40°C (diamonds) and 45°C (inverted triangles).

Table II. Stability parameters of TAA_{UM} and TAA_{MOD}

Methods	TAA_{UM}	TAA_{MOD}
DSC (T_m, °C)	56[a]	64[a]
Far-UV CD (T_m, °C)	52[a],46[b]	86[aU], 84[b]
ANS fluorescence (T_{max}, °C)[c]	50	60
Fluorescence ($[urea]_{1/2}$, M at 40°C)[d]	2.7	4.0
T_{opt} (°C)	50 (50)	50

[a]Unfolding at a scan rate of 60°C h^{-1}; [b]Unfolding at a scan rate of 15°C h^{-1}; [c]Temperature of maximal exposure of hydrophobic residues; [d]Determined by decrease in 330 nm emission at 295 nm excitation. U, T_m underestimated due to the absence of post-transitional baseline. The value in parenthesis was taken from Chang *et al*. (1995).

TAA_{MOD} therefore has greater resistance to unfolding than TAA_{UM} at temperatures between 35°C and 45°C.

TAA_{MOD} has characteristics of an MG

Structural and thermodynamic transitions between folded and unfolded states for both TAA_{UM} and TAA_{MOD} were examined using a variety of experimental techniques. DSC was used to measure transitions during thermal melting. DSC thermograms for both TAA_{UM} and TAA_{MOD} are presented in Fig. 3A. Both forms of TAA show a single endothermic peak (in the absence of deconvolution) in the C_p versus temperature scan, with TAA_{MOD} undergoing a thermal transition at a higher temperature (T_m of 56°C and 64°C for TAA_{UM} and TAA_{MOD}, respectively; Table II). For both TAA_{UM} and TAA_{MOD}, the transitions were irreversible. The peak in heat capacity for TAA_{MOD} is higher and broader than that observed for TAA_{UM}.

In order to determine the structural nature of the thermal transitions, far-UV CD spectroscopy was used to monitor secondary structure as a function of temperature. The CD spectra of both TAA_{UM} and TAA_{MOD} are similar (Supplementary Fig. S3), indicating that in the native state, both TAA_{UM} and TAA_{MOD} have very similar secondary structures.

The ellipticity of TAA_{UM} and TAA_{MOD} at 222 nm, which is a measure of α-helical secondary structure, was recorded as a function of temperature (Fig. 3B). For TAA_{UM}, the curve shows a single-phase transition where the estimated T_m is 52°C, which is close to the temperature at which the thermal transition is observed using DSC. The transition moves from high secondary structure at low temperature to low secondary structure at high temperature, as would be expected for protein unfolding. The transition is irreversible, and hence scan rate dependent.

For TAA_{MOD}, the ellipticity as a function of temperature shows an unusual behaviour (Fig. 3B and C). Between 50°C and 60°C, the ellipticity decreases, indicating an increase in the α-helical content of TAA_{MOD} (Fig. 3C). The curve plateaus followed by a sharp transition to low secondary structure. At a scan rate of 60°C h^{-1} (same rate as the DSC), this second transition did not come to completion, so the transition temperature could only be estimated at >86°C. Because of this, the CD thermal scans for both TAA_{UM} and TAA_{MOD} were repeated at a lower scan rate (15°C h^{-1}), resulting in slightly lower transition temperatures, where all transitions proceed to a plateau, indicating that they are complete (Fig. 3C; Table II).

To directly monitor tertiary structure, the solvent accessibility of hydrophobic residues was measured by monitoring ANS fluorescence as a function of temperature for both TAA_{UM} and TAA_{MOD} (Fig. 3D). A large increase in fluorescence is produced as a result of binding of ANS to the exposed hydrophobic surfaces of a protein molecule. An increased hydrophobic surface can either be inherently present in native cold-adapted enzymes (Georlette *et al*., 2003) or reflects increase in the solvent exposure of nonpolar clusters as a result of MG formation (Kreimer *et al*., 1995; Mizuguchi *et al*., 2005). Although the protein concentration of TAA_{MOD} (41 μg ml^{-1}) was slightly lower than that of TAA_{UM} (45 μg ml^{-1}), the relative fluorescence intensity for the modified enzyme was significantly higher from 20°C to 40°C (Fig. 3D). This suggests greater exposure of nonpolar residues in the modified enzyme. The fluorescence intensity of TAA_{MOD}, increased significantly with an increase in the temperature from 45°C to 65°C, which suggests that the structure has melted into an MG state. On the other hand, there is no large increase in the fluorescence intensity of TAA_{UM} as the temperature goes up, indicating the absence of an MG (Fig. 3D). The peak in ANS fluorescence is used as a measure for the unfolding of the tertiary structure, as ANS gains access to the protein hydrophobic core. For TAA_{UM}, the plot shows an ANS fluorescence maximum at an estimated temperature of 50°C, which is close to the transition temperatures observed by DSC and CD. A clear peak is observed for TAA_{MOD} at ~60°C, which corresponds to the DSC transition and the increase in secondary structure as measured by CD.

Comparing all the data as a function of temperature, it is clear that the thermal transitions observed for TAA_{UM} and

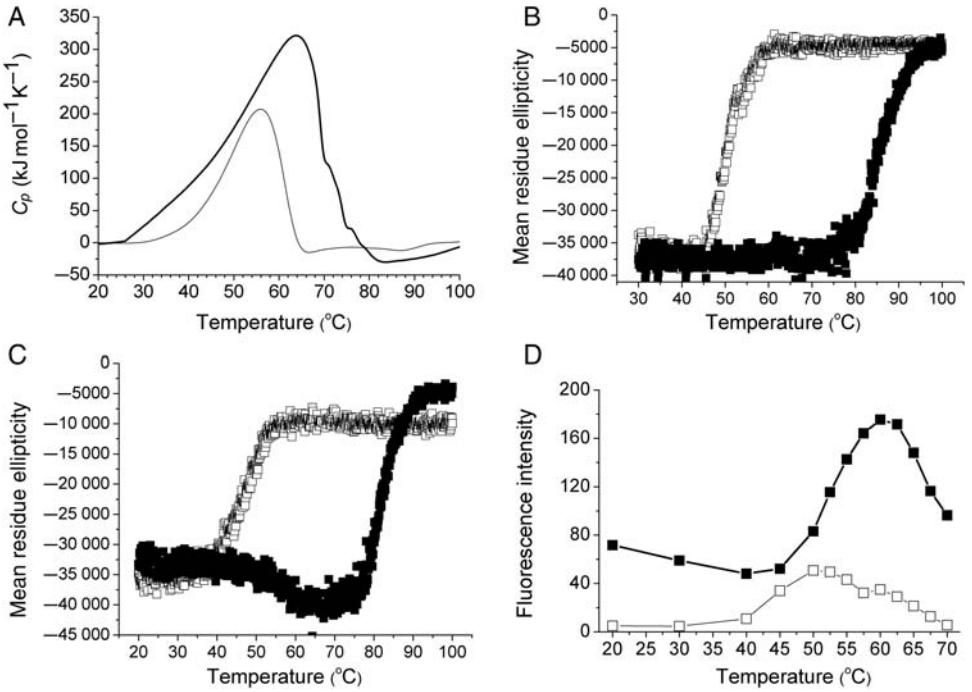

Fig. 3. Thermal properties of TAA_{UM} and TAA_{MOD}. Open symbols or thin line, TAA_{UM}; closed symbols or thick line, TAA_{MOD}. (**A**) Unfolding of tertiary structure using DSC; (**B**) Unfolding of secondary structure using far-UV CD at a scan rate of 60°C h^{-1}; (**C**) Unfolding of secondary structure using far-UV CD at a scan rate of 15°C h^{-1}; (**D**) ANS-fluorescence melting curve.

TAA_{MOD} are of a different nature. The concurrence of the measured T_m by DSC, CD and ANS fluorescence for TAA_{UM} is typical of a globular protein and corresponds to thermal melting from the native to the unfolded state of the protein. In contrast, the behaviour of TAA_{MOD} is atypical. At the transition temperature determined by DSC (C_p), the secondary structure increases (CD measurement, Fig. 3C), whereas the tertiary structure, as measured by ANS fluorescence, is lost. A second transition is observed at ~85°C by CD, where the secondary structure disappears. There is no corresponding peak in the C_p versus temperature thermogram.

These data indicate that at ~65°C, TAA_{MOD} undergoes a transition from the folded state to a state with higher secondary structure, but no tertiary structure. These data are indicative of a transition from a folded state to one which resembles an MG, preserving secondary but not tertiary structure (Ptitsyn, 1995). Similar decreases in ellipticity and increases in α-helical content associated with an MG state have been reported for equinatoxin II, lysozyme and other enzymes (Poklar *et al.*, 1997; Watanabe *et al.*, 2004). At a higher temperature (~85°C), a second transition occurs from the MG state to an unfolded state. There is no corresponding transition observed in the DSC and hence no changes in enthalpy during the transition.

SAXS of TAA_{MOD} reveals that the MG state is compact in 6 M urea

To test whether TAA_{MOD} undergoes a transition from a folded state to an MG-like state, direct structural data were acquired. An MG state should be globular, but somewhat less compact than a native, folded protein. SAXS data provide information about the size, shape and degree of compactness (or 'globularity') of proteins in solution. A range of temperature and urea concentrations were explored to investigate the globularity of TAA_{UM} and TAA_{MOD}. Values of the radius of gyration, R_g, and maximum linear dimension, d_{max}, were either calculated from the TAA crystal structure or experimentally determined by SAXS for TAA_{UM} in the absence of urea and TAA_{MOD} in 6 M urea at 25°C (Table III). The respective $P(r)$ functions are shown in Fig. 4. $P(r)$ is the probable frequency of interatomic vector lengths within the protein and goes to zero at d_{max}. Values of d_{max} were also obtained using the formula

$$d_{max} = \sqrt{12\left(\frac{R_g^2 - R_c^2}{2}\right)} \qquad (8)$$

where R_c is the radius of gyration of the protein cross section. In Equation (8) R_g and R_c were based on the Guinier analyses (Glatter and Kratky, 1982; Guinier and Fournet, 1995).

Table III. R_g and d_{max} values calculated from the TAA crystal structure and experimentally determined by SAXS at 25°C

Sample	R_g (Å)	d_{max} (Å)	Analysis method
TAA_{UM} (crystal structure)	23.8	76	$P(r)$ from model $I(q)$
TAA_{UM} (0 M urea)	23.9 (23.9)	78	$P(r)$ (Guinier)
TAA_{MOD} (6 M urea)	30.2 (30.0)	100	$P(r)$ (Guinier)

The excellent agreement between $P(r)$ functions and structural parameters for the TAA crystal structure and the TAA_{UM} results show that under our experimental conditions TAA_{UM} retains the globular form of the crystal structure. The TAA_{MOD} in 6 M urea at 25°C yields a $P(r)$ with a compact,

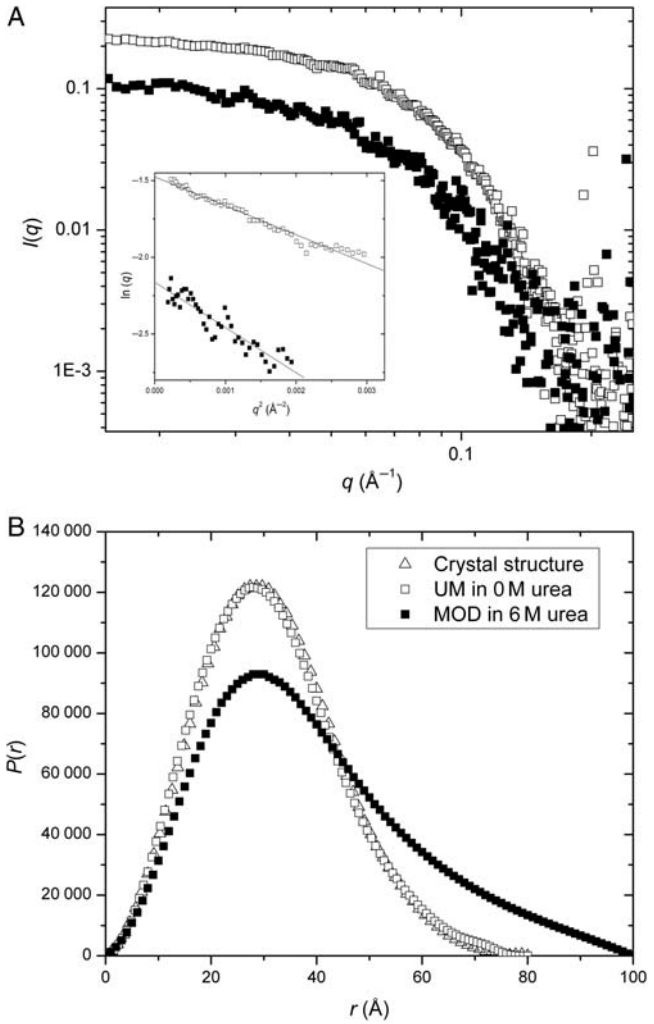

Fig. 4. SAXS of TAA_{UM} and TAA_{MOD}. (**A**) Scattering data as $I(q)$ versus q with the inset showing Guinier plots of the data; (**B**) corresponding $P(r)$ versus r plots. The symbol key for both (A) and (B) is shown in the inset of (B), with TAA_{UM} in the absence of urea and TAA_{MOD} in the presence of 6 M urea, at 25°C.

globular form but with R_g and d_{max} values ~30% larger than the crystal structure, consistent with that expected for the MG state. $I(0)$ of the TAA_{MOD} data suggests the presence of a minor component of aggregation. However, the $P(r)$ shape and the location of the peak are consistent with the results dominated by a single particle form. Additionally, a similar fundamental globular form was observed in TAA_{UM} at 40°C, TAA_{MOD} in 3 M urea at 25°C and TAA_{MOD} in 6 M urea at 40°C, albeit in the presence of clear multiple particle aggregation, precluding a detailed analysis (Supplementary Fig. S4).

X-ray structure of TAA_{MOD} shows that the modifications project into the bulk solvent

The crystal structure of TAA_{MOD} was determined at 2.4 Å resolution (PDB: 3KWX). A model consisting of all native protein atoms (Ala1 to Ser476), a calcium ion, a single *N*-acetyl-D-glucosamine modification to Asn197 and 261 ordered water molecules was refined against the diffraction data (final R-factor of 0.176 with an R-free of 0.211). The refined structure is identical to the published structure of TAA_{UM} (PDB: 2GVY;Vujicic-Zagar and Dijkstra, 2006), with an RMS deviation of 0.28 Å over all 476 Cα atoms comparable with a maximum-likelihood coordinate error of 0.31 Å of the final refined model estimated by phenix refine.

Difference electron density maps showed the presence of modified amino acid side chains. Asn197 shows clear density for a single NAG modification as observed in the structure of the native glycosylated enzyme (Vujicic-Zagar and Dijkstra, 2006). Additional density was observed adjacent to the carboxyl groups of D34, D144, E156, D189, D206, D233, D282, E345 and D355. These difference densities probably indicate that these acidic side chains have been chemically modified (with the exception of either E156 or D233, as these residues are adjacent to the same additional difference density). With the exception of D206, all of these side chains are on the surface of the protein and they are fully solvent exposed. In general, only the amide nitrogen and the first three carbon atoms of the modifying group showed any electron density and hence the map was not good enough for atomic modelling of the modifications. The modifying groups extend into the bulk solvent and they are poorly ordered, having no interactions with the remainder of the protein. There are two exceptions to this: D282 shows potential density (albeit discontinuous) for almost the whole of the arginine methylester modification (Fig. 5A) and significant electron density is observed near the carboxylate of D206 (Fig. 5B). The ordering of the modified D282 is probably due to crystal packing, where the modifying group packs against a symmetry-related protein molecule. The density near D206 is intriguing, as this residue is in the active site of the enzyme. Although the density is strong, it cannot be readily modelled in an unambiguous manner.

In summary, the crystal structure shows that several surface acidic side chains are modified and these modifying groups extend from the protein into the bulk solvent in a disordered fashion. Additionally, D206 in the active site of the protein appears to be modified and this modification occludes part of the active site of the enzyme.

Relationship between high thermostability and reduced entropy of the transition state

To examine whether the higher stability of TAA_{MOD} could be attributed to a reduction in activation entropy ($\Delta S^{\ddagger}$) between the ground state (N) and the partially unfolded transition state ($TS^{\ddagger}$) relative to the transition state of TAA_{UM}, thermodynamic activation parameters of unfolding were derived from DSC thermograms (Fig. 3A) according to the TST as depicted below

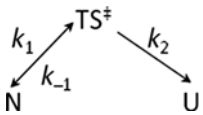

(9)

According to the TST, there is an equilibrium between N and the $TS^{\ddagger}$ and it is important to consider the magnitude of the activation free energy ($\Delta G^{\ddagger}$) barrier between them, which has contributions from both activation enthalpy ($\Delta H^{\ddagger}$) and activation entropy ($\Delta S^{\ddagger}$; Lonhienne *et al.*, 2000). The $\Delta G^{\ddagger}$ was determined as 98 and 100 kJ mol^{-1} for TAA_{UM} and TAA_{MOD}, respectively indicating a higher energy barrier between N and $TS^{\ddagger}$ of TAA_{MOD} when compared with the energy barrier between N and $TS^{\ddagger}$ of TAA_{UM}. From the

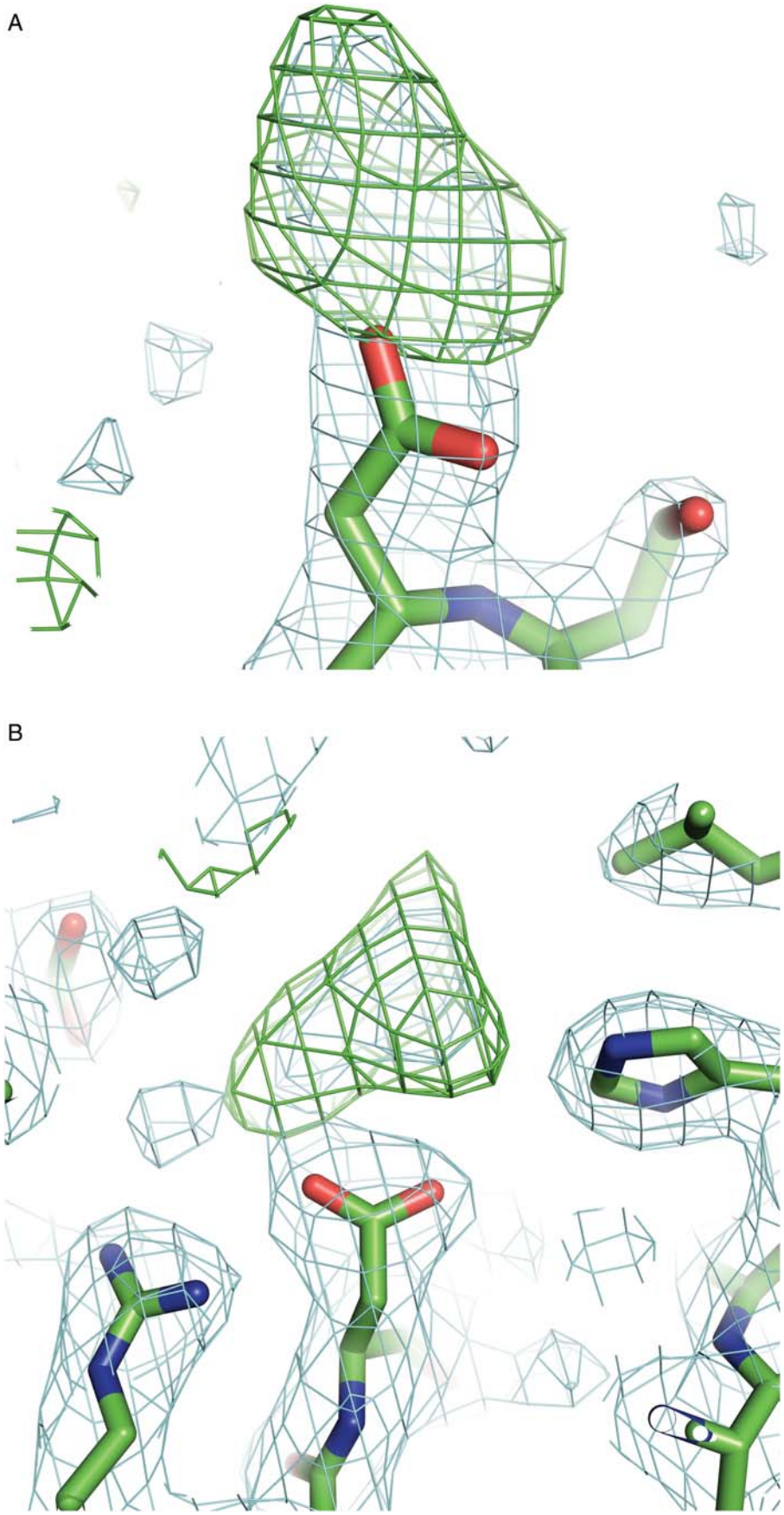

Fig. 5. Electron density maps from the X-ray crystal structure of TAA_{MOD}. Observed electron density ($2F_o - F_c$; light blue mesh; contoured at 1.5 SD) and positive difference density ($F_o - F_c$; green mesh; contoured at 3.5 SD) maps are shown for (**A**) Asp282 and (**B**) Asp206.

Arrhenius plots (Fig. 6), the activation energies of unfolding were determined and $\Delta H^{\ddagger}$ calculated (Segal, 1993; Oliveberg *et al.*, 1995; Siddiqui *et al.*, 2002). The $\Delta H^{\ddagger}$ was 151 ± 1 and 95 ± 3 kJ mol^{-1} for TAA_{UM} and TAA_{MOD}, respectively, whereas $\Delta S^{\ddagger}$ was 164 ± 3 and -15.5 ± 9 J mol^{-1} K^{-1} for TAA_{UM} and TAA_{MOD}, respectively. The increase in the stability of TAA_{MOD} relative to TAA_{UM} is accompanied by a decrease in the values of $\Delta H^{\ddagger}$ and $\Delta S^{\ddagger}$ in accordance with an enthalpy–entropy compensation (Siddiqui and Cavicchioli, 2006). These values indicate that the transition state of TAA_{MOD}, having characteristics of both N and MG, is significantly more structured (ordered) compared with that of TAA_{UM}. These results are similar to other thermally adapted enzymes where the transition states have been reported to be entropically stabilised (D'Amico *et al.*, 2003; Georlette *et al.*, 2003; Siddiqui and Cavicchioli, 2006). The large differences in activation entropy can probably be explained by the fact that the MG state in TAA_{MOD} appears to have more helical content as shown by CD analysis (Fig. 3C). Therefore, the origin of negative entropy observed in TAA_{MOD} could arise if its transition state is more MG-like. Alternatively, negative entropy has been known to occur due to the ordering of solvent molecules on newly exposed hydrophobic surfaces in the transition state (Hurle *et al.*, 1987; Muller, 1992; Shaw and Bott, 1996; Konermann, 2004). This could be the reason for the positive C_p difference observed between TAA_{MOD} and TAA_{UM} at all temperatures during the transition (Fig. 3A), which may be attributed to the additional heat required to disrupt ordered water molecules on the hydrophobic surfaces (Chen and Matthews, 1994; Konermann, 2004; Prabhu and Sharp, 2005). However, caution should be exercised in attributing the difference in C_p of the two proteins to solvent exposure of hydrophobic surface due to the irreversible nature of unfolding.

Kinetics and activation thermodynamics of starch hydrolysis

The kinetic and thermodynamic parameters for starch hydrolysis show that TAA_{MOD} retained 60% starch-hydrolyzing activity at 40°C (TAA_{UM}, k_{cat} 3747 ± 368 min^{-1}; TAA_{MOD}, k_{cat}, 2240 ± 142 min^{-1}). Supplementary Fig. S5 shows the Michaelis–Menten plots. The X-ray structure of TAA_{MOD} showed that the active-site residue, D206, was modified (Fig. 5B). Comparison of peak heights in the electron density map of the modification suggests that ~50% of the protein in the protein crystal was modified at this site. This is consistent with the loss of activity observed for TAA_{MOD}. At 40°C, K_m of TAA_{UM} and TAA_{MOD} was $0.18 \pm 0.04\%$ and $0.13 \pm 0.02\%$ (w/v), respectively. Although no change was observed in relative activation enthalpy ($\Delta\Delta H^{\ddagger}$, 1 kJ mol^{-1}) between TAA_{UM} and TAA_{MOD}; however, decrease in starch-hydrolyzing activity of the modified enzyme was accompanied by a small decrease in activation entropy ($\Delta\Delta S^{\ddagger}$, -8 J mol^{-1} K^{-1}). These data imply that the decrease in the activity of TAA_{MOD} is entropically driven.

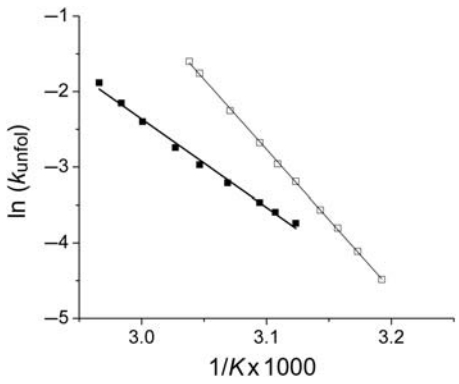

Fig. 6. Arrhenius plots for the determination of activation energies (E_a) for the unfolding of TAA_{UM} and TAA_{MOD}. Thin line, TAA_{UM}; thick line, TAA_{MOD}. R^2 for both plots was >0.99. The errors for both slopes were ± 0.12 and ± 0.36 for TAA_{UM} and TAA_{MOD}, respectively.

Enhanced thermostability leads to increased productivity

For biotechnological purposes, the formation of product or disappearance of substrate over an extended period of time is a superior measure of enzyme performance than initial rate measurements, as the rate of product formation is continuously affected by product/substrate inhibition, enzyme activation and stability (Siddiqui *et al.*, 2009). The altered properties of TAA_{MOD} resulted in the enhanced productivity of starch hydrolysis at a high temperature (60°C; Fig. 7). As the specific activity of TAA_{MOD} was reduced to 60% of TAA_{UM}, the ~2-fold increase in productivity can be attributed to the improved capacity of TAA_{MOD} to resist unfolding at 60°C for extended periods of time (5 h).

Discussion

Our combined data indicate that chemical modification of TAA with AME produced a thermostable MG in which the unfolding of the tertiary structure preceded that of secondary structure by at least 20°C with a concomitant increase in ANS fluorescence relative to the unmodified enzyme. As a result of AME modification, the melting temperature for unfolding of the secondary and tertiary structures of TAA_{MOD} increased by ~34°C and 8°C (Table II), and $t_{1/2\text{-inact}}$ increased 28-fold compared with TAA_{UM} (Table I). We expected that thermostabilisation may have resulted from additional interactions formed by the guanidinium group (e.g. hydrogen bonds, salt bridges or Arg–pi interactions) stabilizing the native state (Mrabet *et al.*, 1992; Gallivan *et al.*, 1999; Siddiqui and Cavicchioli, 2006; Siddiqui *et al.*, 2006). However, the X-ray crystal structure revealed that no crystallographically ordered interactions (electrostatic or other) had resulted from AME modification. This interpretation was supported by the K_{SV} values (16 ± 0.3 M^{-1} at

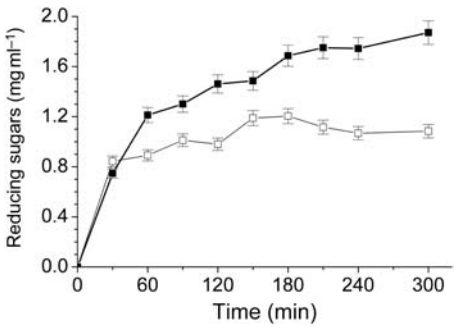

Fig. 7. Productivity of starch hydrolysis at 60°C determined by the formation of reducing sugars. Bars represent the standard error. Thin line, TAA_{UM}; thick line, TAA_{MOD}.

10°C), which indicated that TAA_{UM} and TAA_{MOD} have a similar level of inherent flexibility (Fig. 2B, square).

Stability properties of TAA_{MOD} versus TAA_{UM}

The unfolding of TAA_{MOD} is a two-step process as there exists an intermediate species in the form of an MG, on the unfolding pathway in contrast to one-step unfolding of TAA_{UM}. Rather than being enthalpically induced, the thermodynamic activation parameters indicate that thermostabilisation of TAA_{MOD} has been entropically driven. The entropic stabilisation can be explained by the fact that the MG state of TAA_{MOD} appears to have more helical content than the native state (Fig. 3C). Most studies focusing on improving protein stability have investigated the effects on the native state, and little attention has been directed at the unfolded state or MG state. It is often assumed that the unfolded state possesses no meaningful structure (e.g. random-coil-like state). However, there is good experimental evidence to suggest that under many conditions the unfolded state can maintain residual secondary structure and interactions that promote a compact denatured state or an MG state (Xie and Freire, 1994; Shortle, 1996). On the basis of TST, our data support the stabilisation of TAA_{MOD} resulting from an entropically destabilised transition state.

An alternative way to rationalise the thermodynamic data is to consider the effect of AME modification on the free energy of the folded state N, MG state and unfolded state U, of TAA_{UM} and TAA_{MOD}. Our data indicate that AME modification does not alter the structure of the folded state of TAA_{MOD}. However, the modification results in a change in unfolding pattern, compared with TAA_{UM}, where the latter unfolds irreversibly via a N→U transition, whereas TAA_{MOD}, unfolds in two steps, N→MG→U, with the MG state appearing as the stable form over a significant temperature range. A simple model accounting for these observations is presented in Fig. 8, where the protein can exist in three states, N, MG and U with the only change induced by the AME chemical modification being an increase in the free energy of the unfolded U state. In this model, the MG state is never observed for TAA_{UM}, because an MG state would have a higher free energy than either U or N, whereas for TAA_{MOD} the free energy of U is higher than for TAA_{UM}. TAA_{UM} undergoes a melt from N→U at T_m. However, AME modification causes all three states (N, MG and U) to arise at different temperatures, resulting in two melting temperatures. The first, T'_m, arises from a transition from N→MG, whereas the second transition at a higher temperature, T'_m, results from a transition from MG→U. The first transition (N→MG) of TAA_{MOD} involves an increase in enthalpy as evidenced by the positive peak in the thermogram (Fig. 3A), whereas the second transition (MG→U) does not. With this model, there is no change in the free energy of N, even though T'_m for TAA_{MOD} is higher than T_m for TAA_{UM}. These observations are consistent with the lack of new interactions observed in the X-ray structure. In this model, the only requirement is that AME modification changes the free energy of the unfolded state.

Biotechnological implications of AME-TAA_{MOD}

Improvements made to the productivity, activity or thermostability of enzymes can enhance their commercial value. An additional value will accrue when all enzymes needed for a specific formulation are able to achieve optimal performance under the same reaction conditions (Rivera *et al.*, 2003). TAA_{MOD} exhibits enhanced thermostability that translates to a 200% improvement in starch-hydrolyzing productivity at 60°C (Fig. 7). The magnitude of the increase in thermostabilisation of the secondary structure of TAA_{MOD} (~34°C) is similar to the highest levels previously reported for mutants (that do not form an MG state) generated by directed evolution; a xylanase (ΔT_m, 35°C) and a fungal phytase (ΔT_m, 33°C;Bommarius *et al.*, 2006). Thermostabilisation by AME modification via the novel route of MG formation may provide a useful means for enhancing the value of TAA to biotechnology. Moreover, by better understanding the structure–function–stability relationship of TAA, it may be possible to further engineer improvements.

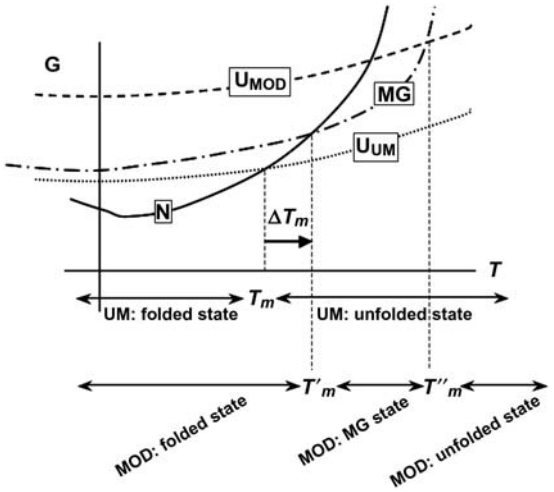

Fig. 8. Model for the effects of chemical modification on TAA. A schematic Gibbs free energy diagram showing $G(T)$ for the folded native state of TAA (N) irrespective of chemical modification, the individual unfolded states of both modified and unmodified TAA (U_{MOD} and U_{UM}, respectively) and the MG state (MG). In this simple model, a change in the Gibbs free energy of the unfolded state caused by chemical modification accounts for the observed thermal melting of both TAA_{MOD} and TAA_{UM}.

Conclusions

Collectively our results show that chemical modification of Taka-amylase by an arginine derivative resulted in a more thermally stable species that unfolds via an MG state. Surprisingly, from the X-ray crystal structure, the Arg modifiers formed no additional permanent electrostatic interactions thus precluding enthalpic factors as the likely cause for stabilisation of the modified enzyme. However, as X-ray crystallography depicts a static structure, one cannot rule out dynamic and transient interactions, or interactions as a result of alternative conformations. Activation thermodynamic analysis showed that the transition state of the modified enzyme was more ordered relative to its native state (negative entropy) probably due to higher secondary structure and/or organization of solvent water molecules on its exposed hydrophobic surface.

Supplementary data

Supplementary data are available at *PEDS* online.

Acknowledgements

The help of Stephen Harrop and Paul Curmi in acquisition and analysis of X-ray diffraction data is gratefully acknowledged. We are thankful to the referees for improving the manuscript with their valuable comments.

Funding

This work was supported by the Australian Research Council (ARC). Mass spectrometric results were obtained at the Bioanalytical Mass Spectrometry Facility within the Analytical Centre of the University of New South Wales. This work was undertaken using infrastructure provided by NSW Government co-investment in the National Collaborative Research Infrastructure Scheme (NCRIS). Subsidised access to this facility is gratefully acknowledged.

References

Adams,P.D., Grosse-Kunstleve,R.W. and Hung,L.W., *et al*. (2002) *Acta Crystallogr. D Biol. Crystallogr.*, **58**, 1948–1954.
Bommarius,A.S., Broering,J.M., Chaparro-Riggers,J.F. and Polizzi,K.M. (2006) *Curr. Opin. Biotechnol.*, **17**, 606–610.
Brzozowski,A.M. and Davies,G.J. (1997) *Biochemistry*, **36**, 10837–10845.
Cavicchioli,R.C., Curmi,P.M.G., Siddiqui,K.S. and Thomas,T. (2006) In Rainey,F.A. and Oren,A. (eds), *Methods in Microbiology.* Academic Press, Elsevier Ltd, UK, pp. 395–436.
Chang,C.T., Tang,M.S. and Lin,C.F. (1995) *Biochem. Mol. Biol. Int.*, **36**, 185–193.
Chen,X. and Matthews,C.R. (1994) *Biochemistry*, **33**, 6356–6362.
Collaborative Computational Project. (1994) *Acta Crystallogr. D Biol. Crystallogr.*, **50**, 760–763.
Cox,J.M., Davis,C.A., Chan,C., Jourden,M.J., Jorjorian,A.D., Brym,M.J., Snider,M.J., Borders,C.L., Jr and Edmiston,P.L. (2003) *Biochemistry*, **42**, 1863–1871.
D'Amico,S., Marx,J.C., Gerday,C. and Feller,G. (2003) *J. Biol. Chem.*, **278**, 7891–7896.
Daniel,R.M., Danson,M.J., Hough,D.W., Lee,C.K., Peterson,M.E. and Cowan,D.A. (2008) In Siddiqui,K.S. and Thomas,T. (eds), *Protein Adaptation in Extremophiles.* Nova Science Publishers, New York, USA, pp. 1–34.
Dolginova,E.A., Roth,E., Silman,I. and Weiner,L.M. (1992) *Biochemistry*, **31**, 12248–12254.
Duy,C. and Fitter,J. (2005) *J. Biol. Chem.*, **280**, 37360–37365.
Eijsink,V.G., Bjørk,A., Gåseidnes,S., Sirevåg,R., Synstad,B., van den Burg,B. and Vriend,G. (2004) *J. Biotechnol.*, **113**, 105–120.
Emsley,P. and Cowtan,K. (2004) *Acta Crystallogr. D Biol. Crystallogr.*, **60**, 2126–2132.
Fitter,J. (2005) *Cell. Mol. Life Sci.*, **62**, 1925–1937.
Fitter,J. and Haber-Pohlmeier,S. (2004) *Biochemistry*, **43**, 9589–9599.
Fritz,G., Bergmann,A. and Glatter,O. (2000) *J. Chem. Phys.*, **113**, 9733–9740.
Fukada,H., Takahashi,K. and Sturtevant,J.M. (1987) *Biochemistry*, **26**, 4063–4068.
Gallivan,J.P. and Dougherty,D.A. (1999) *Proc. Natl Acad. Sci. USA*, **96**, 9459–9464.
Georlette,D., Damien,B., Blaise,V., Depiereux,E., Uversky,V.N., Gerday,C. and Feller,G. (2003) *J. Biol. Chem.*, **278**, 37015–37023.
Glatter,O. and Kratky,O. (1982) *Small Angle X-Ray Scattering.* Academic Press, London.
Guinier,A. and Fournet,G. (1995) *Small Angle Scattering of X-Rays.* John Wiley and Sons, New York.
Hurle,M.R., Michelotti,G.A., Crisanti,M.M. and Matthews,C.R. (1987) *Proteins*, **2**, 54–63.
Janecek,S. and Baláz,S. (1992) *FEBS Lett.*, **304**, 1–3.
Jeffries,C.M., Whitten,A.E., Harris,S.P. and Trewhella,J. (2008) *J. Mol. Biol.*, **377**, 1186–1199.
Konermann,L. (2004) *Encyclopedia of Life Sciences.* John Wiley and Sons, New York, pp. 1–6.
Koshiba,T., Yao,M., Kobashigawa,Y., Demura,M., Nakagawa,A., Tanaka,I., Kuwajima,K. and Nitta,K. (2000) *Biochemistry*, **39**, 3248–3257.
Kreimer,D.I., Shnyrov,V.L., Villar,E., Silman,I. and Weiner,L. (1995) *Protein Sci.*, **4**, 2349–2357.
Lonhienne,T., Gerday,C. and Feller,G. (2000) *Biochim. Biophys. Acta*, **1543**, 1–10.
Matsumura,M., Signor,G. and Matthews,B.W. (1989) *Nature*, **342**, 291–293.
McCoy,A.J., Grosse-Kunstleve,R.W., Adams,P.D., Winn,M.D., Storoni,L.C. and Read,R.J. (2007) *J. Appl. Crystallogr.*, **40**, 658–674.
Mitidieri,S., Martinelli,A.H.S., Schrank,A. and Vainstein,M.H. (2006) *Bioresour. Technol.*, **97**, 1217–1224.
Mizuguchi,M., Matsuura,A. and Nabeshima,Y., *et al*. (2005) *Proteins*, **61**, 356–365.
Mrabet,N.T., Van den Broeck,A. and Van den brande,I., *et al*. (1992) *Biochemistry*, **31**, 2239–2253.
Muller,N. (1992) *TIBS*, **17**, 459–463.
Oliveberg,M., Tan,Y-J. and Fersht,A.R. (1995) *Proc. Natl Acad. Sci. USA*, **92**, 8926–8929.
Petsko,G.A. (2001) *Methods Enzymol.*, **334**, 469–478.
Poklar,N., Lah,J., Salobar,M., Macek,P. and Vesnaver,G. (1997) *Biochemistry*, **36**, 14345–14352.
Prabhu,N.V. and Sharp,K.A. (2005) *Annu. Rev. Phys. Chem.*, **56**, 521–548.
Ptitsyn,O.B. (1995) *TIBS*, **20**, 376–379.
Ptitsyn,O.B. (1996) *Nat. Struct. Biol.*, **3**, 488–490.
Richardson,T.H., Tan,X. and Frey,G., *et al*. (2002) *J. Biol. Chem.*, **277**, 26501–26507.
Rivera,M.H., López-Munguía,A., Soberón,X. and Saab-Rincón,G. (2003) *Protein Eng.*, **16**, 505–514.
Sanchez-Ruiz,J.M., Lopez-Lacomba,M.C., Cortijo,M. and Mateo,P.L. (1988) *Biochemistry*, **27**, 1648–1652.
Segal,I.H. (1993) *Enzyme Kinetics: Behavior and Analysis of Rapid Equilibrium and Steady-State Enzyme Systems*. John Wiley and Sons, New York.
Shaw,A. and Bott,R. (1996) *Curr. Opin. Struct. Biol.*, **6**, 546–550.
Shokri,M.M., Khajeh,K., Alikhajeh,J., Asoodeh,A., Ranjbar,B., Hosseinkhani,S. and Sadeghi,M. (2006) *Biophys. Chem.*, **122**, 58–65.
Shortle,D. (1996) *FASEB J.*, **10**, 27–34.
Siddiqui,K.S. and Cavicchioli,R. (2005) *Extremophiles*, **9**, 471–476.
Siddiqui,K.S. and Cavicchioli,R. (2006) *Annu. Rev. Biochem.*, **75**, 403–433.
Siddiqui,K.S., Loviny-Anderton,T., Rangarajan,M. and Hartley,B.S. (1993) *Biochem. J.*, **296**, 685–691.
Siddiqui,K.S., Cavicchioli,R. and Thomas,T. (2002) *Extremophiles*, **6**, 143–150.
Siddiqui,K.S., Poljak,A. and Cavicchioli,R. (2004) *Cell. Mol. Biol.*, **50**, 657–667.
Siddiqui,K.S., Poljak,A. and Guilhaus,M., *et al*. (2006) *Proteins*, **64**, 486–501.
Siddiqui,K.S., Parkin,D.M., Curmi,P.M.G., De Francisci,D., Poljak,A., Barrow,K., Noble,M.H., Trewhella,J. and Cavicchioli,R. (2009) *Biotechnol. Bioeng.*, **103**, 676–686.
Stanley,S.M. and Poljak,A. (2003) *J. Chromatogr. B*, **785**, 205–218.
Svergun,D. (1992) *J. Appl. Cryst.*, **25**, 495–503.
Svergun,D.I., Barberato,C. and Koch,M.H.J. (1995) *J. Appl. Cryst.*, **28**, 768–773.
Uversky,V.N. (2002) *Protein Sci.*, **11**, 739–756.
Vieille,C. and Zeikus,G.J. (2001) *Microbiol. Mol. Biol. Rev.*, **65**, 1–43.
Violet,M. and Meunier,C. (1989) *Biochem. J.*, **263**, 665–670.
Vujicic-Zagar,A. and Dijkstra,B.W. (2006) *Acta Crystallogr. Sect. F*, **62**, 716–721.
Walker,J.M. (2002) *The Protein Protocols Handbook*. Humana Press, NJ, USA.
Wang,C., Lascu,I. and Giartosio,A. (1998) *Biochemistry*, **37**, 8457–8464.
Watanabe,M., Kobashigawa,Y., Aizawa,T., Demura,M. and Nitta,K. (2004) *Protein J.*, **23**, 335–342.
Xie,D. and Freire,E. (1994) *Proteins*, **19**, 291–301.
Xie,Q., Guo,T., Lu,J. and Zhou,H.M. (2004) *Int. J. Biochem. Cell. Biol.*, **36**, 296–306.
Zhang,N., Suen,W.C., Windsor,W., Xiao,L., Madison,V. and Zaks,A. (2003) *Protein Eng.*, **16**, 599–605.